Identifying the modal properties of nonlinear structures using measured free response time histories from a scanning laser Doppler vibrometer

Michael W. Sracic
Department of Engineering Physics
University of Wisconsin-Madison
mwsracic@gmail.com

Matthew S. Allen
Department of Engineering Physics
University of Wisconsin-Madison
Madison, WI 53706
msallen@engr.wisc.edu

Hartono Sumali
Component Science and Mechanics
Sandia National Laboratories
Albuquerque, NM 87185
hsumali@sandia.gov

ABSTRACT

This paper explores methods that can be used to characterize weakly nonlinear systems, whose natural frequencies and damping ratios change with response amplitude. The focus is on high order systems that may have several modes although each with a distinct natural frequency. Interactions between modes are not addressed. This type of analysis may be appropriate, for example, for structural dynamic systems that exhibit damping that depends on the response amplitude due to friction in bolted joints. This causes the free-response of the system to seem to have damping ratios (and to a lesser extent natural frequencies) that change slowly with time. Several techniques have been proposed to characterize systems such systems. This work compares a few available methods, focusing on their applicability to real measurements from multi-degree-of-freedom systems. A beam with several small links connected by simple bolted joints was used to evaluate the available methods. The system was excited by impulse and the velocity response was measured with a scanning laser Doppler vibrometer. Several state of the art procedures were then used to process the nonlinear free responses and their features were compared. First the Zeroed Early Time FFT technique was used to qualitatively evaluate the responses. Then, the Empirical Mode Decomposition method and a simple approach based on band pass filtering were both employed to obtain monocomponent signals from the measured responses. Once monocomponent signals had been obtained, they were processed with the Hilbert transform approach, with several enhancements made to minimize the effects of noise.

1. Introduction

Many built-up systems consist of substructures that are assembled with bolted joints. Although some significant strides have been made in recent years, it is still exceedingly difficult to predict the nonlinear damping behavior of bolted joints, caused by micro- and macro-slip in the bolted joint interfaces. New experimental methods are needed to allow one to characterize the nonlinear damping in real structures so better models can be created. In the recent literature, researchers have applied several approaches in order to identify nonlinear damping from structures. The most common approach involves using some form of time-frequency analysis [1]. For example, the Hilbert transform [2, 3] has been widely used to estimate the instantaneous frequency and phase of a signal.

This method is quite satisfactory for single frequency component signals of single degree-of-freedom systems. Furthermore, the method is extended to multi-frequency component signals with the Hilbert-Huang transform, which uses Empirical Mode Decomposition [4] to decompose the original response into several single frequency component signals. In a more recent paper [5], the authors relate the Empirical Mode Decomposition approach to the analytical slow flow analysis, and this approach provides a theoretical basis that promises to extend these concepts to multi-degree of freedom nonlinear systems. The wavelet transform is an alternative to the Hilbert-Huang approach. In [6], the authors used the wavelet transform to analyze free-decay time responses of a built-up beam system, but this type of analysis becomes challenging if the damping is not very light or if the nonlinearity is strong causing the spectra to become difficult to interpret visually. Kerschen et al. [7] have proposed an important extension to this approach where the system is excited at a specific nonlinear normal mode and allowed to freely decay along that mode. A controlled input (e.g. a sinusoidal input from a shaker) is typically required. However, attaching a shaker adds mass and damping to the structure and inhibits its free response.

Several methods have been suggested to identify joint properties using measured frequency response functions, for example [8-11]. However, these methods may be sensitive to measurement noise, may only provide valid models for certain frequency ranges, or may require one to assume some information regarding the model for the joints a priori. In any event, these approaches rely on linear theory, so they don't seem to be able to predict the amplitude dependent damping that is characteristic of many systems with bolted joints.

While several methods are available to identify nonlinear models of systems with bolted joints, all of the available methods have limitations and none has proved to be the best method in all situations. Furthermore, few of the methods have been applied to real measurements from high order systems. This work will compare several of the most promising methods in order to evaluate their relative merits. In order to ground the comparison in a real, yet relatively simple system, a test structure was created that consists of a free-free steel beam (i.e. suspended with elastic strings) with several steel links attached. The links are bolted to the beam in various combinations using various torque values, and the beam is excited by an impulsive force and allowed to freely vibrate while its velocity response is measured with a scanning laser Doppler vibrometer (SLDV). The SLDV is non-contact, so the ring-down responses are not affected by the sensor. The time response is recorded as the beam freely vibrates. Additionally, the linear frequency response function is also estimated using the impulsive force, which was also measured. Both the time histories and linear frequency response functions are used to characterize the damping of this high order nonlinear system. First, standard experimental modal analysis is performed and the best-fit linear damping is extracted at different bolt torques in order to get a baseline linear approximation of the damping trends for different torques. Then, the time histories are interrogated using both the Hilbert-Huang Transform with Empirical Mode Decomposition and single-mode band-pass filtering, in order to isolate individual frequency component signals (Intrinsic Mode Functions). In the end, a curve-fitting procedure that was presented in [12] is used to fit the nonlinear time dependent properties of the Intrinsic Mode Function, and the nonlinear time dependent frequency and damping is extracted. The rest of this paper will review the theory for the methods that will be used, introduce the linked-beam experiment, show and discuss the results from when the proposed methods are applied to the responses from the experiment, and discuss and present some conclusions based on the applied techniques.

2. Theory

The free response of a general nonlinear system can be represented by the following state space equation

$$y(t) = f(x, t) \tag{1}$$

where x(t) is the time dependent state vector and f is a nonlinear function that describes how the state and input combine to define the response. The function f is assumed to be sufficiently smooth so that all partial derivatives are well defined. When this is the case, the system can be linearized about specific points in the state space or about entire trajectories (e.g. periodic orbits [13]). In general the linearized modes of a nonlinear system interact and exchange energy, so one must consider all of the linearized modes and their nonlinear couplings to construct the free response. Indeed, this characteristic has even been exploited to create a very effective nonlinear vibration absorber [14]. On the other hand, systems with weak nonlinearities are frequently observed to have insignificant modal interactions, in which case the free response can be expressed as follows. Let the response y(t) define the free-decay velocity of the system such that $y_i(t) = v_i(t)$ is the j^{th} measured velocity, which conforms to

the property just described. From here forward, the response v(t) will be assumed to be from the j^{th} degree of freedom and the subscript will be dropped. Then, for a quasi-linear system (i.e. a nonlinear system with smooth nonlinearities that vary slowly with time), the free decay velocity can be represented with the following equation

$$y_{j}(t) = v(t) = \sum_{r=1}^{m} A_{r}(t) \cos(\omega_{d,r}t + \varphi_{0,r})$$
 (2)

where m is the number of frequencies present in the response, $A_r(t)$ is the time varying amplitude for the r^{th} frequency component, $\omega_{d,r}$ is the r^{th} damped natural frequency, and $\varphi_{0,r}$ is the r^{th} phase variable. If the response is linear, then the frequency will be constant and the amplitude given by $A_r(t) = A_0 e^{-\zeta_r \omega_{n,r} t}$, where $\omega_{n,r}$ is the natural frequency and is related to the damped natural frequency by $\omega_{d,r} = \omega_{n,r} \sqrt{1-\zeta^2}$. If the velocity response is nonlinear, then the damped natural frequency and hence the argument of the cosine function may vary with time and the amplitude may not be a simple exponential. The experimental methods of interest in this work seek to characterize the time dependent frequency and damping in order to obtain the amplitude-frequency and amplitude-damping relationships for the system.

Although it will not be pursued in this work due to space limitations, the complexification approach discussed in Kerschen et al. can be used to compute the time varying amplitude and frequency of a nonlinear system from its equation of motion, establishing a more solid theoretical foundation for eq. (2).

2.1 Zeroed-Early Time Fast Fourier Transform

The first method considered is the Zeroed early-time fast Fourier transform (ZEFFT) that was presented recently by Allen & Mayes [15]. This frequency domain technique was shown to be quite effective at detecting nonlinearity even in relatively high order systems with quite severe nonlinearities. This method is briefly reviewed below.

For many systems, nonlinearities are only present when the system responds with large amplitude, so the response becomes more linear as the response amplitude diminishes. At very low amplitude one may reach a point where the response is linear so that the free response can be written as

$$v(t) = \sum_{r=1}^{m} R_r \exp(\lambda_r t) + R_r^* \exp(\lambda_r^* t)$$
(3)

where R_r and λ_r are the r^{th} residue and eigenvalue, respectively, and the complex conjugate is denoted with ()*. If the system has under-damped modes, then the complex conjugate eigenvalue pairs are defined by $\lambda_r = -\zeta_r \omega_{n,r} + i\omega_{d,r} \text{ where the coefficient of critical damping, } \zeta_r \text{, has been introduced and } i = \sqrt{-1} \text{.}$ The Fourier transform can be used to compute the frequency domain counterpart to Eq. (3) (assuming that the response is zero for t<0).

$$V(\omega) = \sum_{r=1}^{m} \frac{R_r}{i\omega - \lambda_r} + \frac{R_r^*}{i\omega - \lambda_r^*}$$
(4)

As described in [15], this is identical to the expression for the frequency response of a linear system in terms of its modes, except that the residues in eq. (4) have a different definition than the residues of a linear frequency response function. Even then, the spectrum has the same shape as the frequency response of a linear mode near each natural frequency.

Now if the signal is artificially set to zero up to a certain time denoted t_z (i.e. $v_z(t)=0$ for $t < t_z$ and $v_z(t)=v(t)$ otherwise), then the Fourier transform of $v_z(t)$ is

$$V_z(\omega) = \sum_{r=1}^m \left(\frac{R_r e^{\lambda_r t_z}}{i\omega - \lambda_r} + \frac{(R_r e^{\lambda_r t_z})^*}{i\omega - \lambda_r^*} \right) e^{i\omega t_z}$$
(5)

and the residues change to reflect the initial value of the response at time t_z but otherwise the spectrum has approximately the same shape, especially near the peaks. If the spectra are compared for various zero times (various amounts of the initial response erased) one would see peaks that have essentially the same shape but with decreasing amplitude.

On the other hand, if the system has the nonlinearity that was described previously then the influence of the nonlinearity will diminish as t_z increases, and when one compares $V(\omega)$ and $V_z(\omega)$ the spectrum will show that the effective frequency (and perhaps damping) of the system has changed. Plots of the spectra versus the truncation time, t_z , give a qualitative description of the nonlinearity in the system. The method can be extended to give quantitative measures of nonlinearity (i.e. using the backwards extrapolation for nonlinearity detection (BEND) technique described in [15]), although in this work it will be used primarily to detect nonlinearity and evaluate it qualitatively.

2.2 Hilbert-Transform

Slow-flow analysis is often realized through the Hilbert transform, which can be applied as follows. First, the discrete-time analytic signal is formed by augmenting the real response signal v(t) with its Hilbert transform $\widetilde{v}(t)$ as follows.

$$V(t) = v(t) + i\tilde{v}(t) \tag{6}$$

Note that in this case, the signal v(t) is assumed to be mono-component (contain only one frequency component), so the 'r' subscript is dropped from these equations. The magnitude of the analytic signal, |V(t)|, is the envelope of the response. If the signal is monocomponent then the envelope can be readily related to the damping in the system.

$$A(t) = |V(t)| \tag{7}$$

Assuming that the damping and frequency are slowly varying functions of time, the amplitude or decay envelope can be estimated as the following

$$A(t) = A_0 \exp(-\zeta(t)\omega_n(t))$$
(8)

where A_0 is the initial amplitude, and the natural frequency $\omega_n(t)$ and coefficient of critical damping $\zeta(t)$ are both functions of time for a general nonlinear system. The phase can be obtained from the analytic form of the measured signal (i.e. Eq. (6)) using the following equation.

$$\varphi(t) = \tan^{-1}\left(\tilde{v}(t) / v(t)\right) \tag{9}$$

In order to obtain the damped natural frequency, some authors have time-differentiated the phase signal [2]. However, most measured signals contain a certain amount of noise which can corrupt the time-differentiated signal. Following [12], an alternative approach is to use the measured response at time instants $t = t_0, t_1, \dots, t_{N-1}$, (N = 0 number of data points) and fit the phase signal $\varphi(t)$ with a polynomial of degree, p.

$$\begin{cases}
\varphi(t_{0}) \\
\varphi(t_{1}) \\
\vdots \\
\varphi(t_{N-1})
\end{cases} = \begin{bmatrix}
t_{0}^{p} & \cdots & t_{0} & 1 \\
t_{1}^{p} & \cdots & t_{1} & 1 \\
\vdots & \cdots & \vdots & 1 \\
t_{N-1}^{p} & \cdots & t_{N-1} & 1
\end{bmatrix} \begin{bmatrix} b_{p} \\
\vdots \\
b_{1} \\
b_{0} \end{bmatrix}$$
(10)

The polynomial coefficients b_0, b_1, \ldots, b_p can be obtained by a least squares solution of the above system of equations. Then, since the instantaneous frequency is the time derivative of the phase, the time-varying damped oscillation frequency can be estimated as the time-derivative of the previous equation.

$$\omega_{d}(t) = \frac{d\varphi(t)}{dt} = \begin{bmatrix} pt_{0}^{p-1} & \cdots & 1 & 0 \\ pt_{1}^{p-1} & \cdots & 1 & 0 \\ \vdots & \cdots & \vdots & \vdots \\ pt_{N-1}^{p-1} & \cdots & 1 & 0 \end{bmatrix} \begin{bmatrix} b_{p} \\ \vdots \\ b_{1} \\ b_{0} \end{bmatrix}$$
(11)

The next step is to estimate the decay envelope. Again, assuming that the signal is nonlinear, the decay envelope will be time varying and can be well approximated with a polynomial. The coefficients of the polynomial can be calculated from the following equation (assuming a third order polynomial).

$$\begin{cases}
\ln |V(t_0)| \\
\ln |V(t_1)| \\
\vdots \\
\ln |V(t_{N-1})|
\end{cases} = \begin{bmatrix}
t_0^3 & t_0^2 & t_0 & 1 \\
t_1^3 & t_1^2 & t_1 & 1 \\
\vdots & \vdots & \vdots & \vdots \\
t_{N-1}^3 & t_{N-1}^2 & t_{N-1} & 1
\end{bmatrix} \begin{bmatrix} c_3 \\ c_2 \\ c_1 \\ \ln (A_0) \end{bmatrix} \tag{12}$$

Now the above cubic regression analysis gives a nonlinearly decaying envelope,

$$A(t) = A_0 \exp\left(-c_1 t - c_2 t^2 - c_3 t^3\right)$$
(13)

which implies that the following relationship holds.

$$\zeta(t)\omega_n(t) \equiv C(t) = \left(c_1 + c_2 t + c_3 t^2\right) \tag{14}$$

Then, using the relationship between the damped natural frequency, the natural frequency, and the coefficient of critical damping, $(\omega_d(t))^2 = (\omega_n(t))^2 \left(1 - (\zeta(t))^2\right)$, the time-varying natural frequency $\omega_n(t)$ can be computed.

$$\omega_{\rm n}(t) = \sqrt{\left(\omega_{\rm d}(t)\right)^2 + \left(C(t)\right)^2} \tag{15}$$

Finally, the time-varying damping ratio $\zeta(t)$ can be computed.

$$\zeta(t) = \frac{-C(t)}{\omega_n(t)} \tag{16}$$

If the measured response is linear, then only the linear terms will be significant in the polynomial regressions in Eqs. (10-12), and the procedure identifies the constant linear natural frequency and coefficient of critical damping.

2.3 Empirical Mode Decomposition

In general the response of a nonlinear system is composed of oscillations of multiple different frequencies, so the method in the previous section cannot be directly applied. One must first isolate individual oscillatory components (often called intrinsic mode functions or IMFs) so that their time varying frequency and damping can be characterized. The Empirical Mode Decomposition method was developed to isolate the intrinsic mode functions, which are constrained to obey two properties. For each intrinsic mode function, the number of local extrema and the number of zero crossings must be equal or differ by no more than one. Additionally, the envelopes defined by the local maxima and the local minima must have a mean of zero. Using these two properties, the IMFs can be successively removed from the full, multi-component signal with an iterative process, which is well described in a few references [1, 16]. To start the process, the measured response (i.e. v(t)) is interrogated for its local maxima and minima. A cubic spline is fit to the local maxima and then to the local minima to form the upper and lower envelops, respectively. Then, the mean of these curves is calculated and designated as m_1 . The first estimate for the IMF is formed by subtracting the mean signal from the original signal.

$$h_1 = v(t) - m_1 \tag{17}$$

The estimate may need to be refined in order to satisfy the intrinsic mode function criteria, so one iterates on the estimate by repeating the previous process until the k^{th} IMF estimate

$$h_{1k} = h_{1(k-1)} - m_{1k} (18)$$

satisfies the criteria for an intrinsic mode function. Then, the first intrinsic mode function $c_1 = h_{1k}$ can be subtracted from the original signal

$$r_1 = v(t) - c_1 \tag{19}$$

In order to start sifting for the remaining IMFs, the procedure is repeated now using the residual signals (i.e. $r_2 = r_1 - c_2$, ..., $r_m = r_{m-1} - c_m$). Once the m^{th} residual r_m is monotonic, or has only one local extremum [16], then the decomposition is complete. The procedure is ad hoc, in general, but it often works quite well and, as was shown in [5], it can be directly linked to the theoretical slow-flow analysis.

3. Experimental application to linked-beam system

As mentioned previously, a structure was designed in order to evaluate these methods. The structure was designed to have the following features:

- Numerous modes in the 0-2000Hz range.
- o The modes are well separated in frequency.
- Modular attachments can be bolted to the main structure in various combinations to vary the nonlinear damping.
- The attachments do not cause modes to switch order (e.g., the third lowest mode in frequency should remain the third no matter which links are attached). This feature would allow modal damping to be more easily related to the combination of attachments.
- o The structure can be assembled and disassembled with good repeatability.
- o The joints can be readily modeled with sufficient detail using the finite element method (FEM).
- The structure can be modeled analytically with reasonable accuracy.
- The structure can be accurately measured with out-of-plane scanning LDV (so data from many measurement points could be obtained without modifying the structure).

Figure 1 shows a schematic of the beam and three links that were bolted to the beam. The beam was 508mm long, 50.8mm wide, and 6.35mm thick. Six through-holes were drilled on the beam's midline for $\frac{1}{4}$ -inch fine-thread bolts, which were used to attach the three links. The bolt hole pattern started at 63.5mm from one end, and the spacing between holes was 76.2mm. The three links were 12.7mm wide and 3.175mm thick. Through-holes were also drilled near the ends of the links for the $\frac{1}{4}$ -inch bolts. The links were fastened to the beam with

the bolts and a washer between each pair of facing surfaces. All parts of the structure were made of AISI 304 stainless steel. All mating surfaces on the beam and on the links were polished to a roughness of 0.1 micron or smoother.

The experiment was designed to minimize the effects of the boundary conditions on the measured damping. A clamped boundary condition, for example, would cause significant damping at the clamp which could dominate the measured damping and make it difficult to calculate the damping caused by the bolted joints. Thus, a free-free boundary condition was chosen. The beam was excited by impacts in order to avoid using excitation hardware with surfaces that rub such as those of attached force transducers and stingers. The cables required to attach conventional sensors (e.g. accelerometers) can also introduce damping so the vibration responses were measured with a laser Doppler vibrometer.

The finite element method (FEM) was used to predict the natural frequencies and mode shapes of the structure. Because FEM modal analysis cannot account for nonlinear rubbing interfaces, the interfaces were fused together in the model so that the whole built-up structure was modelled as monolithic. The FEM model was used to iterate the design towards the features mentioned above.

While the structure was designed to allow various combinations of link attachments, this paper discusses only a case where all three links are bolted to the beam. To characterize the effects of bolt torques on modal damping, the torque on all the six bolts was varied using 9.04 Nm (80 Lbf.in), 10.2 Nm (90 Lbf.in), and 12.4 Nm (110 Lbf.in).

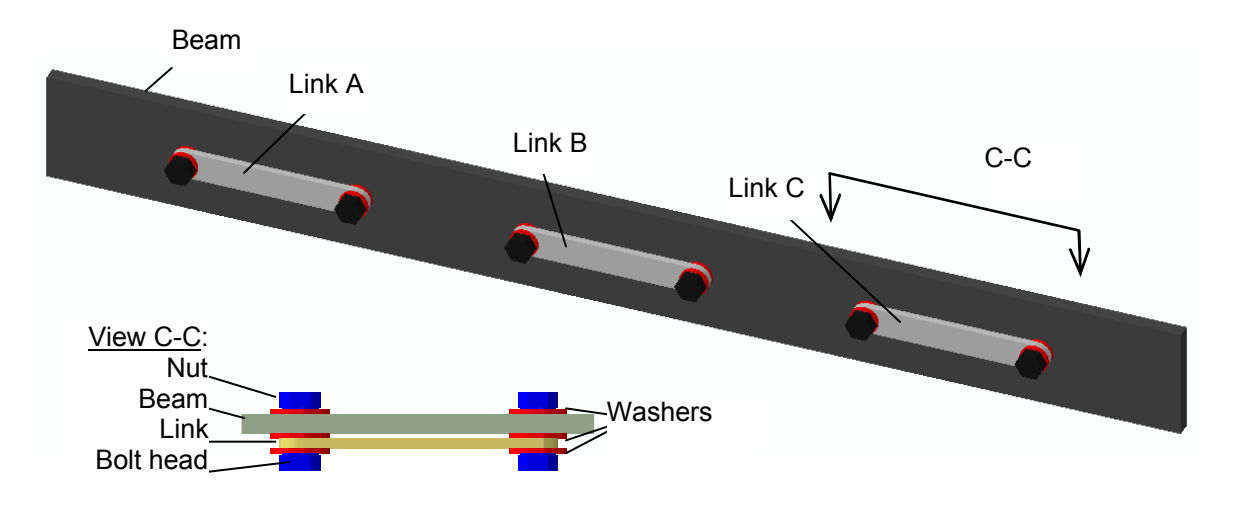
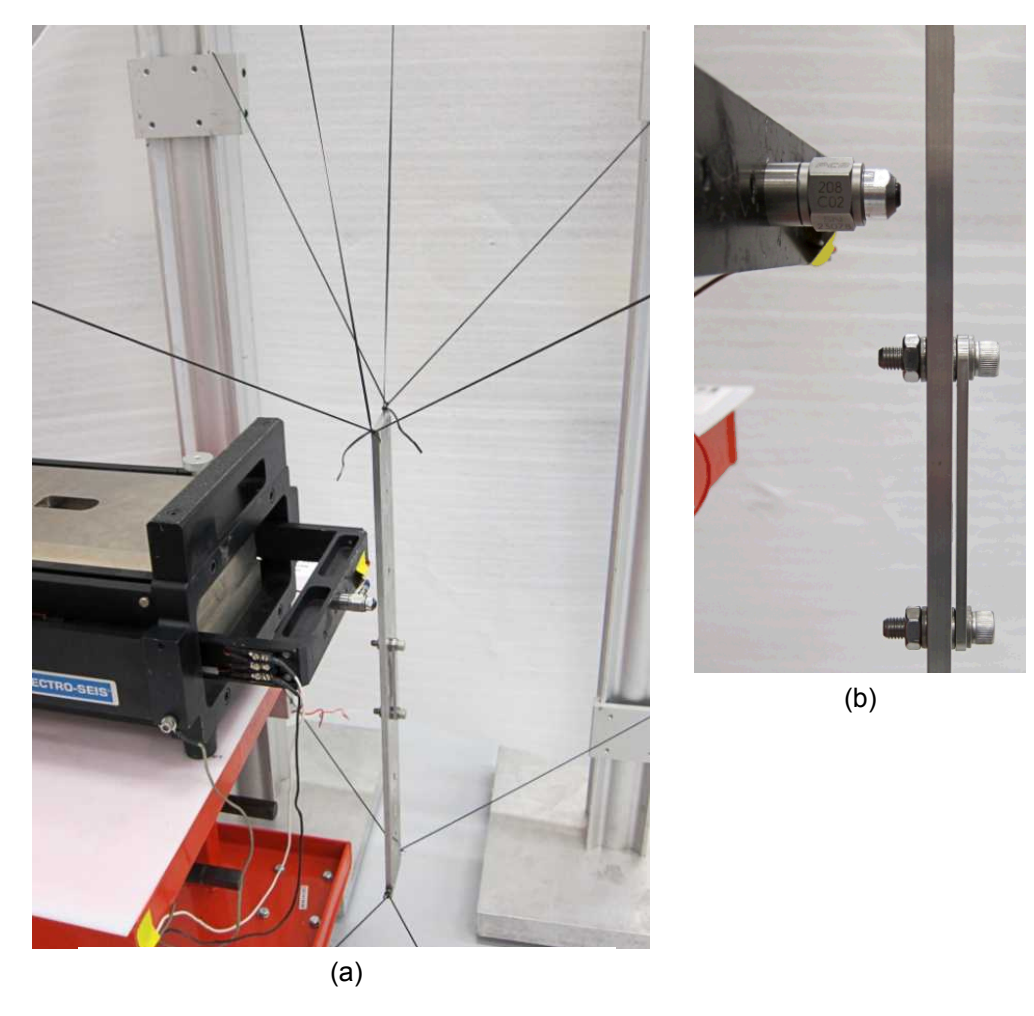


Figure 1: Finite element model of the linked-beam

3.1 Experiment

The beam was suspended in a manner that emulated the free-free boundary condition as shown in Fig. (1a). Two strings suspended the beam from overhead points. Four elastic strings kept the beam from swinging too much out-of-plane since that would cause the laser spot to depart from the measurement point of interest. A small patch of retro-reflective tape was adhered to the beam at each measurement point (see Fig. (3)). These patches ensured that the LDV sensor received adequate light even if the test article rotated relative to the laser.



Fiure 2: (a) Test structure suspended by two vertical in-plane strings and four out-of-plane elastic strings, and (b) Close up showing the beam, one link with its bolted joints, and the force transducer on the shaker armature

The structure was excited with an impulsive force from a shaker-impactor as follows. An APS 400 long-stroke shaker carried a force transducer at the end of its armature. A special waveform command was designed and applied to the amplifier, which caused the shaker to push the force transducer into the beam then to retract quickly after impact. The force transducer was then held in the retracted position so that the swinging of the beam did not cause a second impact. After the rigid-body deflections of the structure dissipated, the shaker brought the force transducer close to the structure again and the process was repeated.

The peak force of the impact was around 150N. Upon each impact, the laser Doppler vibrometer (LDV) computed the mobility (frequency response function) between the input and response. The sampling rate of 12800 samples/second gave a bandwidth of 5000Hz. The scanning LDV recorded the mobility at 63 points shown in Fig. (3) using four averages at each point. The impact location was behind point 28. Point 22 was on link B, and point 53 was on the main beam.

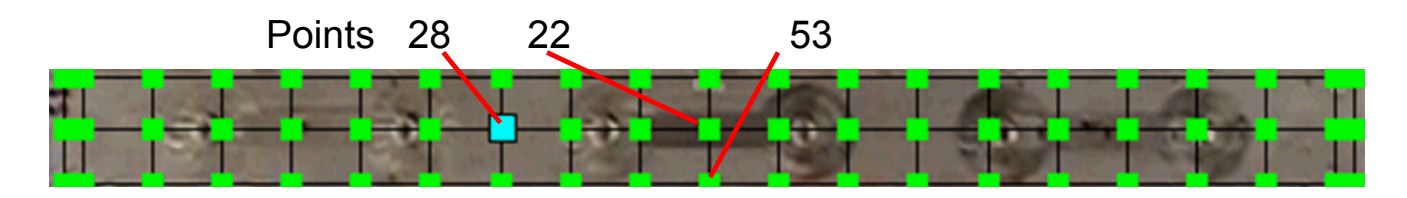


Figure 3: Laser Doppler vibrometer scan points on the structure

3.2 Nonlinearity Detection with Zeroed-Early Time Fast Fourier Transforms

The measurements were first interrogated using the Zeroed Early-time FFT (ZEFFT) method [15], in order to obtain a qualitative understanding of the degree to which the structure is behaving nonlinearly. The measurements with the bolts at a torque of 10.2 Nm were first investigated. There were 62 measurement points, so the ZEFFTs of the entire dataset were computed and the average of the magnitude of the ZEFFTs was computed over all of the measurement points for each zero time. Figure 4 shows the resulting average spectrum for various values of t_z . The system is predominantly linear, so the spectrum near each peak must be closely examined to see any sign of nonlinearity. Figures 5 and 6 show expanded views near the 1st and 3rd bending modes respectively. The former shows that the first natural frequency appears to be constant, within the resolution of the measurement at least. The third natural frequency seems to show a very small shift from 801.1 Hz to 801.5 Hz (at t_z =1.2 sec. or later). All of the other peaks were similarly inspected and small, 0.5 Hz frequency shifts were also noticeable in the modes at 1192 Hz and 2871 Hz. All of the other peaks seemed to have constant frequencies.

While this analysis suggests that the frequencies of these modes remain essentially constant, visual inspection does not reveal whether the damping is changing nonlinearly. The BEND procedure described by Allen & Mayes [15] could be used to assess this to some extent, although this will not be pursued in this work. Since the nonlinearity seems to be quite weak, it might be reasonable to approximate this system as linear. This is explored in the following section.

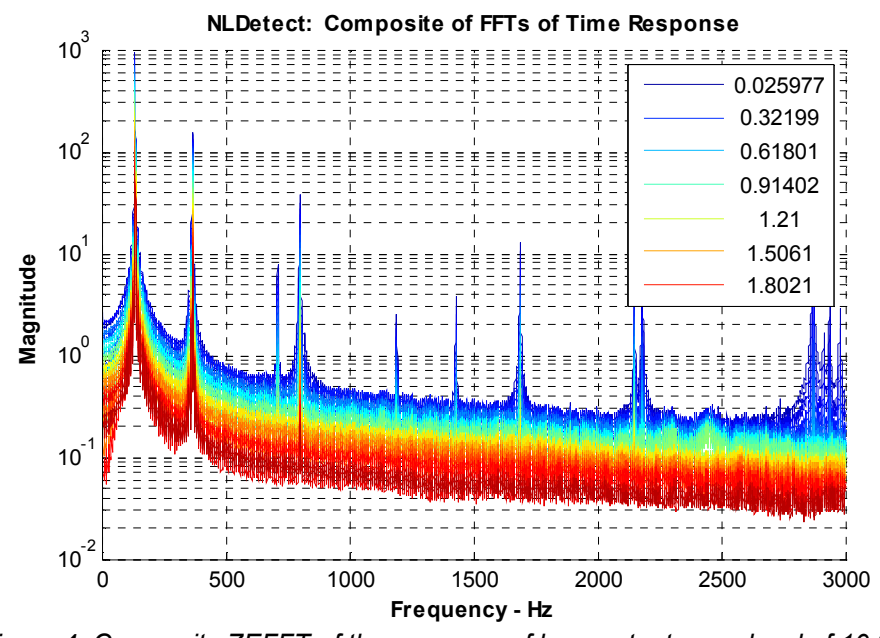


Figure 4: Composite ZEFFT of the response of beam at a torque level of 10.2 Nm

3.3 Linear Modal Analysis Using Low-Excitation Frequency Response Functions

Since the ZEFFT method showed weak evidence of nonlinearity, the standard approach using linear modal analysis was first attempted to see whether a linear model might be adequate to characterize the system at each torque value. This section discusses results from a separate modal test where the peak impact force was 50N instead of 150N. The purpose of the test was to investigate the effect of bolt torques on linearized damping. The LDV software computes an 'average spectrum', which is an average of the mobilities at all the scanned points. The resonant frequencies of the structure correspond to the peaks of the average spectrum. In this paper, those peaks will be called 'peaks of average mobility' (PAM). The PAM gives a good estimate of the natural frequencies of the structure. These estimates were useful in determining poles in the linear experimental modal analysis (EMA). The LDV software also plotted the mobility values at all scanned points at a chosen frequency. At each PAM, the spatial distribution of those mobility values (i.e. operating deflection shape) gives a good estimate of the mode shape since none of the modes have close natural frequencies.

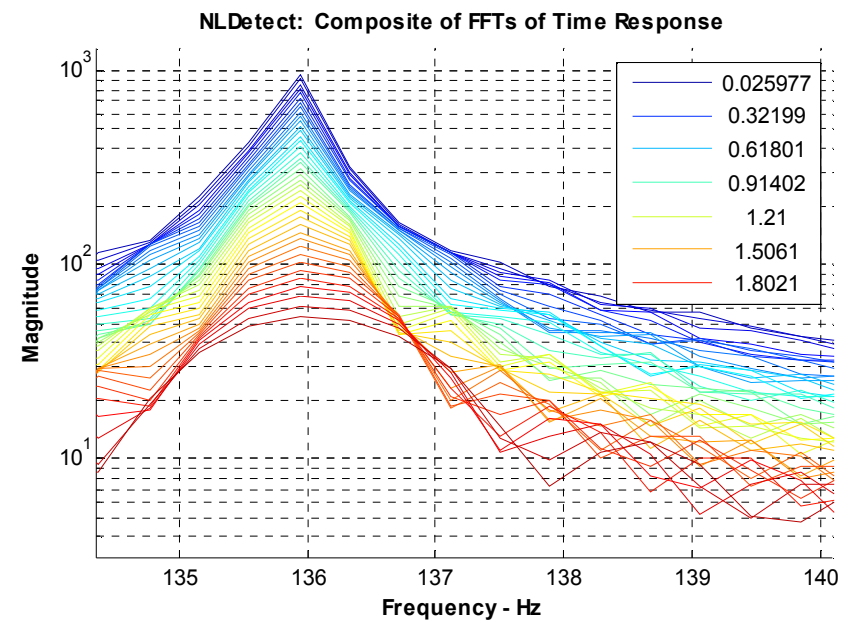


Figure 5: Expanded view of Figure 4 near the natural frequency of the first bending mode

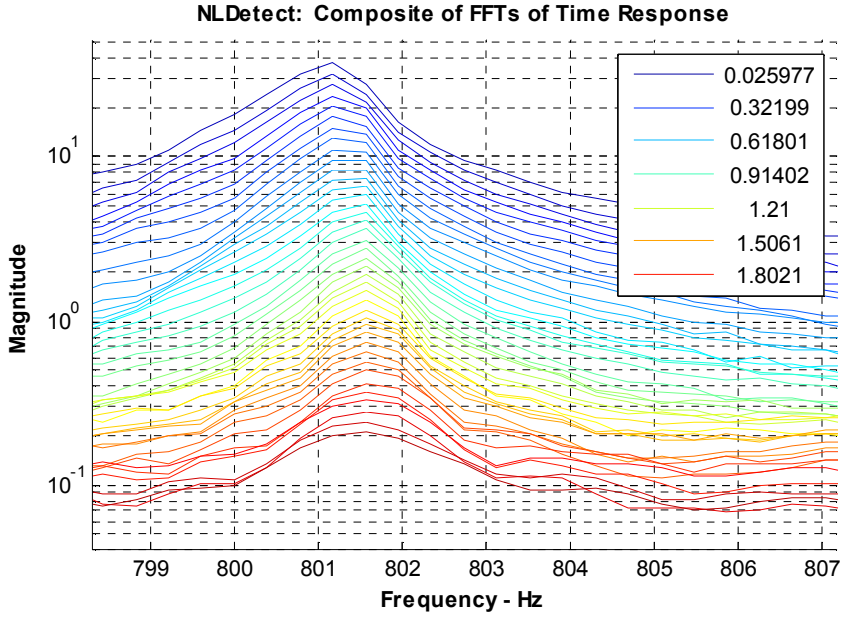


Figure 6: Expanded view of Figure 4 near the natural frequency of the third bending mode

Linear curve fitting was performed using accelerances (computed from the mobilities) from the measurements at each torque level. ATA Engineering's AFPoly software was used to perform the curve fitting. The low end of the analysis frequency band was set to 30Hz to exclude all rigid-body modes caused by the soft free-free suspension cords. The mode indicator function (MIF) and 'stability' diagram showed estimates of where the natural frequencies are likely to be. In almost all cases, the peaks of the MIF were collocated with the trains of poles on the stability diagram. These frequencies were very close to the PAM from the LDV software. Thus, for the most part the EMA was straightforward. Appendix 1 shows the MIF and stability diagram, along with sketches of the mode shapes. Near 2500Hz and 4000Hz there is strong indication of a mode. However, observation of the shape from the PAM led to the conclusion that the modes around those two frequencies involve primarily in-plane motion. Because the links were attached to only one side of the beam, the in-plane motion resulted in a little out-of plane motion. Those modes are probably not well measured by the laser and hence will not be analyzed here.

EMA was difficult near certain frequencies because the three nominally identical links resonate at similar frequencies. The combinations of one, two and three links resonating together created a high modal density; five modes were found between 2870Hz and 3015Hz. In that range, the PAM and stability diagram had to be used together to identify the modes. Despite the high modal density, the five modes in that range were identified. For example, Fig. (7) shows good agreement between accelerances from measurement (solid curves) and from the synthesis (dashed curves) of the identified modes for the bolt torque case of 9.04 Nm. A careful comparison does show differences between the reconstruction and the measurements that are on the order of 10% of the peak, but differences such as this can arise for many reasons and they are not large enough that one would typically call the linear model into question.

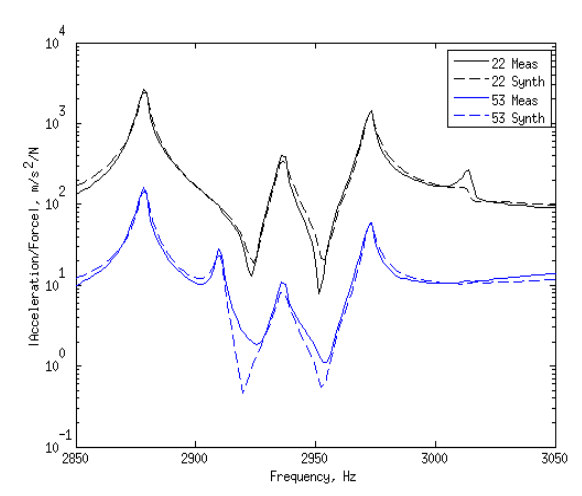


Figure 7: Accelerances at points 22 (higher magnitudes) and 53 (lower magnitudes) in the 2850 to 3050 Hz range for bolt torque case 9.04 Nm; Solid curves are from measurements; dashed curves are AFPoly synthesis

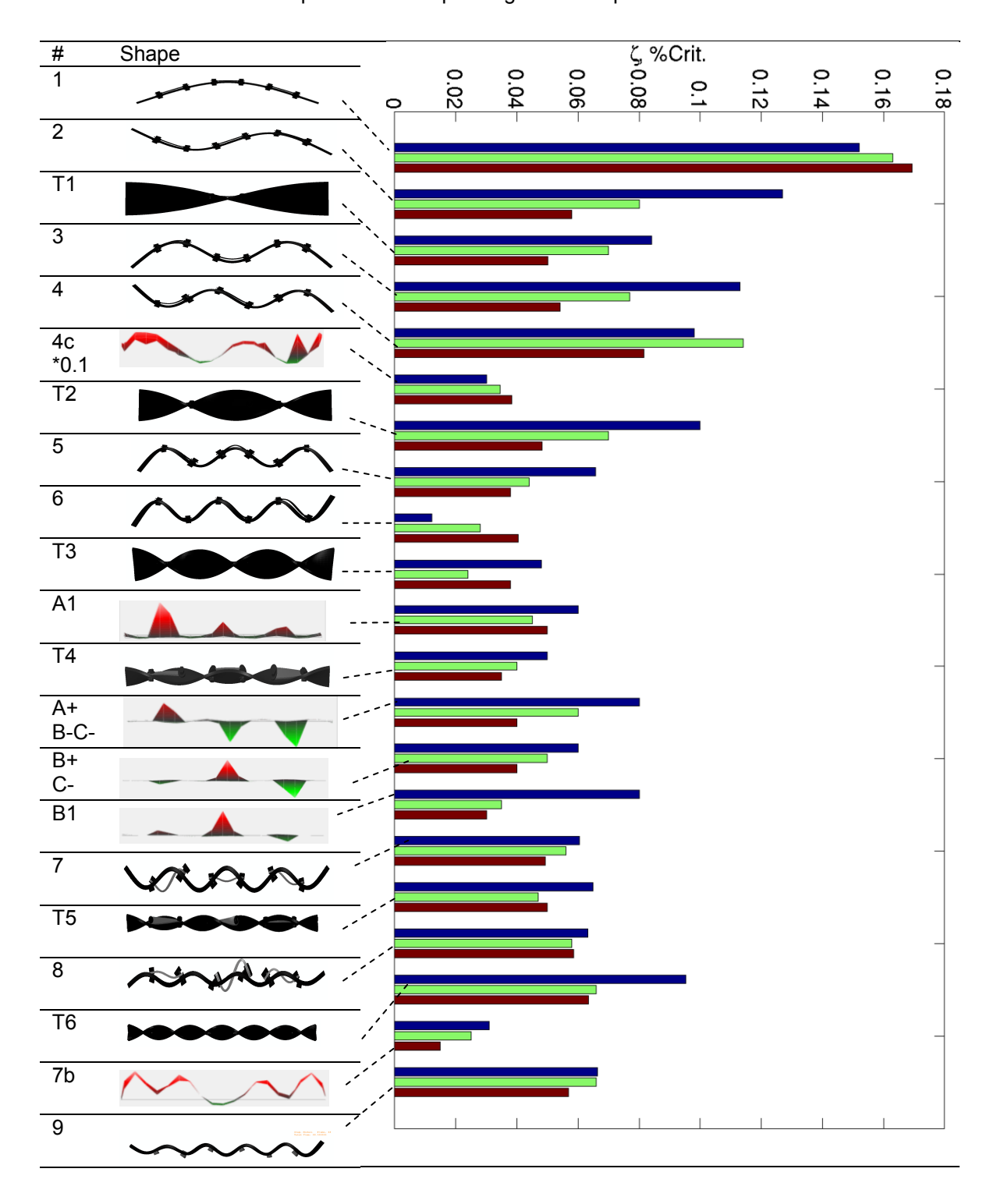
Table 1 shows the modal damping ratios for 21 modes with three bolt torques: 'low' torque of 9.04 Nm, 'medium torque' of 10.2 Nm, and 'high' torque of 12.4 Nm. The plots of most of the mode shapes are from a finite element analysis (FEA). The rest of the plots (modes 4c, A1, etc.) came from the spatial distribution of mobility amplitudes at the PAM, because the monolithic FEA did not predict those modes. (The modes in question seemed to depend strongly on the characteristics of the interfaces in the joints.) The modes are shown in Table 1 from top to bottom in the order of increasing natural frequencies. The bars in the chart show the identified linear modal damping of each mode as percentage of critical damping. Three bars are shown for each mode: the bar on the top represents damping for the low bolt torque, the middle bar for the medium torque, and the bottom bar for the high torque.

Mode 4c had much higher damping than the rest of the modes, so its damping was multiplied by 0.1 prior to displaying it on the plot. This mode is of questionable accuracy; its shape is very similar to mode 4, but it has a strong local motion of link C. This mode could be an artifact caused by processing nonlinear measurements with linear frequency response estimation and modal analysis procedures.

Using Table 1, one can assess the effect of bolt torques on modal damping. The damping for these 13 modes clearly decreases as the bolt torques increase. In five other modes, the low torque still gives higher damping than the high torque, but the medium torque gives the lowest or highest damping among the three torques. Three modes (1, 4c and 6) exhibit damping that increases with higher torque, which is the opposite trend from other modes.

Table 1: Beam with three links ABC, various bolt torques.

- Bar chart on the right depicts the critical damping ratio for each mode for low torque = 9.04 Nm (blue bar), medium torque = 10.2 Nm (green bar), and high torque = 12.4 Nm (red bar).
- Mode 4c was much more heavily damped than the rest, so its damping ratios were multiplied by 0.1 in order to fit on the bar chart.
- The table on the left depicts the corresponding mode shapes.



3.4 Nonlinear Modal Analysis Using Free Ring-down History

The linear modal analysis in the preceding section gave an estimate of the modal damping of the structure. The following section discusses three techniques to study the *nonlinear* damping. The free response velocity due to 150N peak impacts was measured at each of the points in Fig. (3) for 2.56 seconds at all three of the torque levels. Figure 8 shows the response at the torque level of 10.2 Nm for point 28, which is at the same location as the impactor. The dashed blue curve is the measured response. There is a considerable amount of low frequency vibration in the response (likely due to rigid body motion of the beam on the suspension system). The response was high-pass filtered with an 8th order Butterworth filter and a cut off frequency of 30 Hz. The filtered response is plotted with the red curve, which seems to remove the low frequency motion.

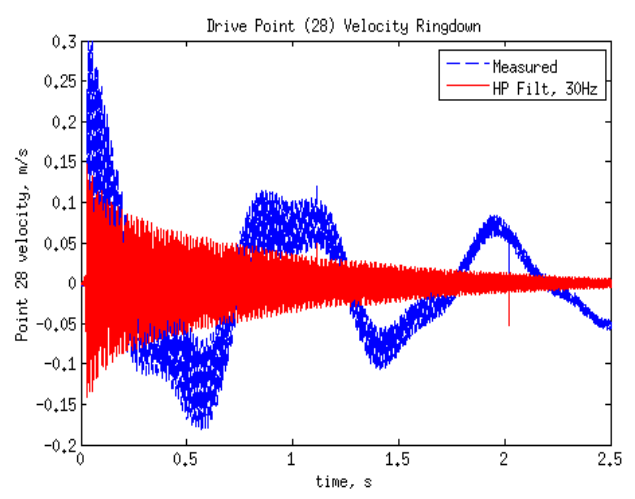


Figure 8 Free velocity response of point 28: measured (dashed blue), high-pass filtered with a 30 Hz cut off frequency (red)

This signal will be used as a benchmark in this paper, although there were many other measurement points available. The bolted joints in this beam provide very complicated nonlinear damping relationships, and before the spatial information provided by the numerous measurement points can be taken into account we seek first to characterize a single response. Figure 9 shows the FFT magnitude of the velocity response of point 28 (after filtering and drop out bridging). There are many sharp peaks in the response out to 12 kHz, so the signal certainly has multiple frequency components.

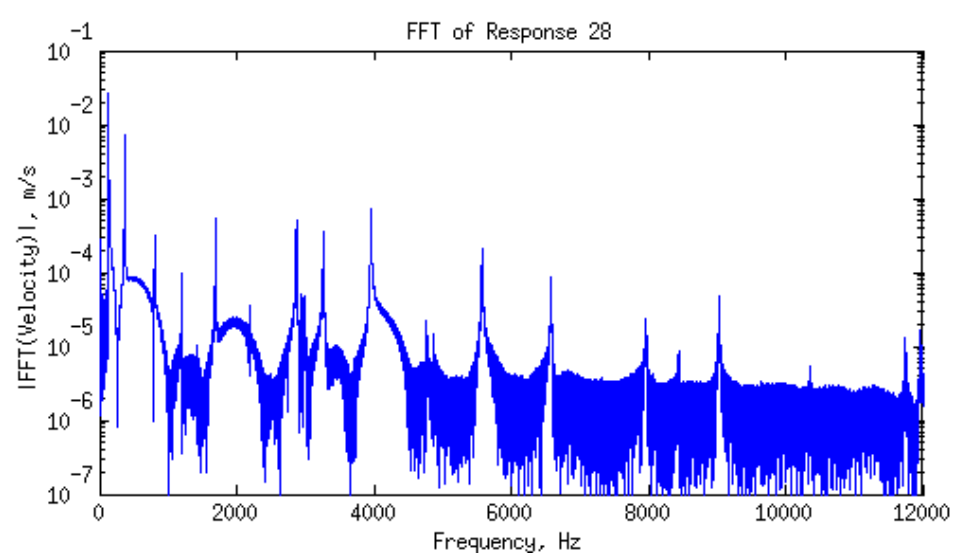


Figure 9: FFT magnitude of the free velocity response of point 28

The response of point 28 is characteristic of many of the responses measured on the beam. There are many modes involved in each response, but most of the modes are well separated. The goal is to determine which

modes contain nonlinearity and to try to identify the time dependent properties of those nonlinearities. Since the free velocity response contains multiple significant modes, it is necessary to first isolate mono-component signals which contain the time dependent properties of a single mode.

3.4.1 Application of Empirical Mode Decomposition

In order to isolate mono-component signals, the Empirical Mode Decomposition (EMD) method was applied to the free velocity response. For this paper, the EMD implementation from Ortigueira that is available on MATLAB Centrals File exchange was used, and this algorithm was based on Rato 2008. The EMD procedure extracted 12 intrinsic mode functions (IMFs) from the free velocity response. Figure 10 shows plots of the first three IMFs. The time domain signals are plotted in 10a, and the frequency domain signals are plotted in 10b from 0-7000 Hz. The spectra of the first IMF (top plot of (b)) still contains several significant peaks near 4000, 5600, and 6600 Hz as well as several less coherent peaks at lower frequencies. The spectrum of the second IMF contains one dominant peak near 400 Hz, and the third IMF contains two dominant peaks near 130 Hz and 360 Hz.

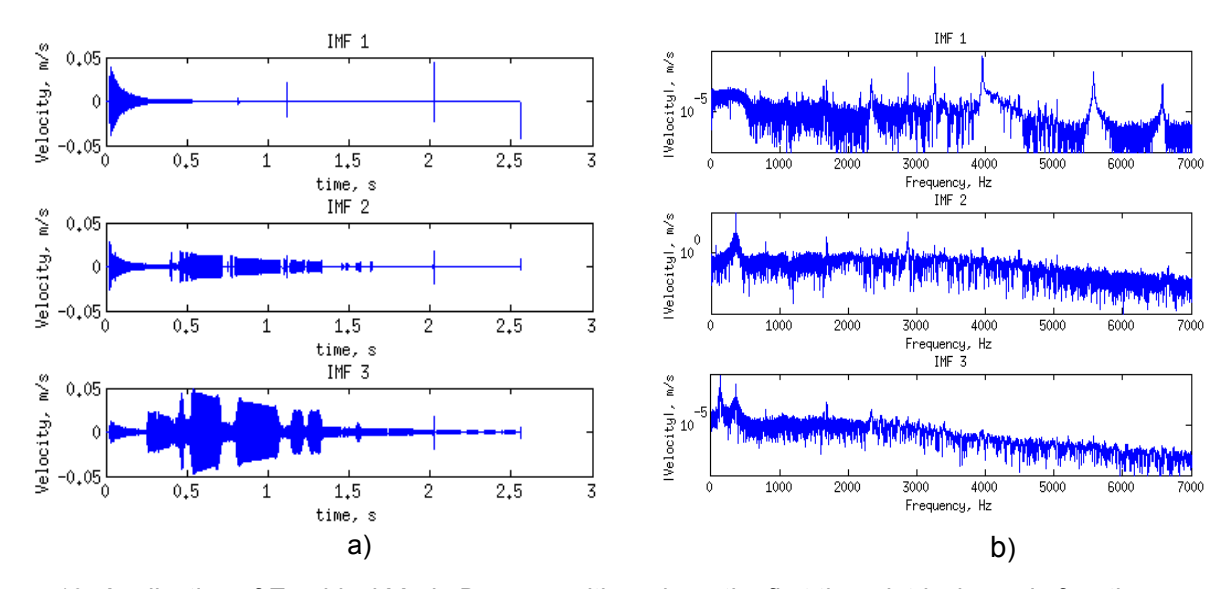


Figure 10: Application of Empirical Mode Decomposition where the first three intrinsic mode functions are shown:

a) time domain; b) frequency domain

The EMD algorithm sifted through the components of the free velocity response and extacted several signals that contained significantly less frequency content. The second IMF, for example, seems to contain only one major component. However, as seen in the first and third IMF, the signals still contain the effects of several modes. Moreover, the EMD process adds a certain amount of broad band noise to the responses, which can be seen in the frequency spectra of the IMF signals.

Since there are numerous modes in the free velocity response, it is possible that the EMD procedure has difficulty isolating all of the individual components. The algorithm may perform better if the response was first low-pass or high-pass filtered to reduce the number of modes that need to be separated. The authors are exploring these ideas, but the Hilbert transform method used in this paper performs best when the signal contains only one frequency component, so the EMD signals were not processed further. Instead, a different sifting procedure was implemented as described in the next section.

3.4.2 Band-pass Filtering of Individual Modes

Next, the authors applied a single mode filtering procedure where different Butterworth filters were applied to the time domain free velocity response in order to isolate individual frequency components in the signal. The ZEFFT analysis did not show much frequency shift in any of the modes, so the stiffness of the system is predominantly linear. Hence, it is unlikely that any of the modes contain harmonic peaks at higher frequencies, but the spectra can always be visually scanned to see if this type of the nonlinear phenomenon is occurring. The free velocity response did not show signs of harmonics of any of the modes occurring at higher frequencies, so it was assumed that each mode could be isolated with a single bandpass filter. Figure 11 shows the results when the first two modes were isolated using this filtering procedure. First, the free velocity response was filtered with a 10th order

low-pass Butterworth filter with a cut-off frequency of 240 Hz. The frequency spectra of the measured signal and the filtered signal are shown in Fig. 11(a). The filtered time domain signal is shown in 11(b). In order to isolate the second mode, the measured signal was filtered with a 5th order band-pass Butterworth filter with cut-off frequencies of 300 and 450 Hz. The frequency spectra and the time domain response are shown in 11(b) and (c), respectively.

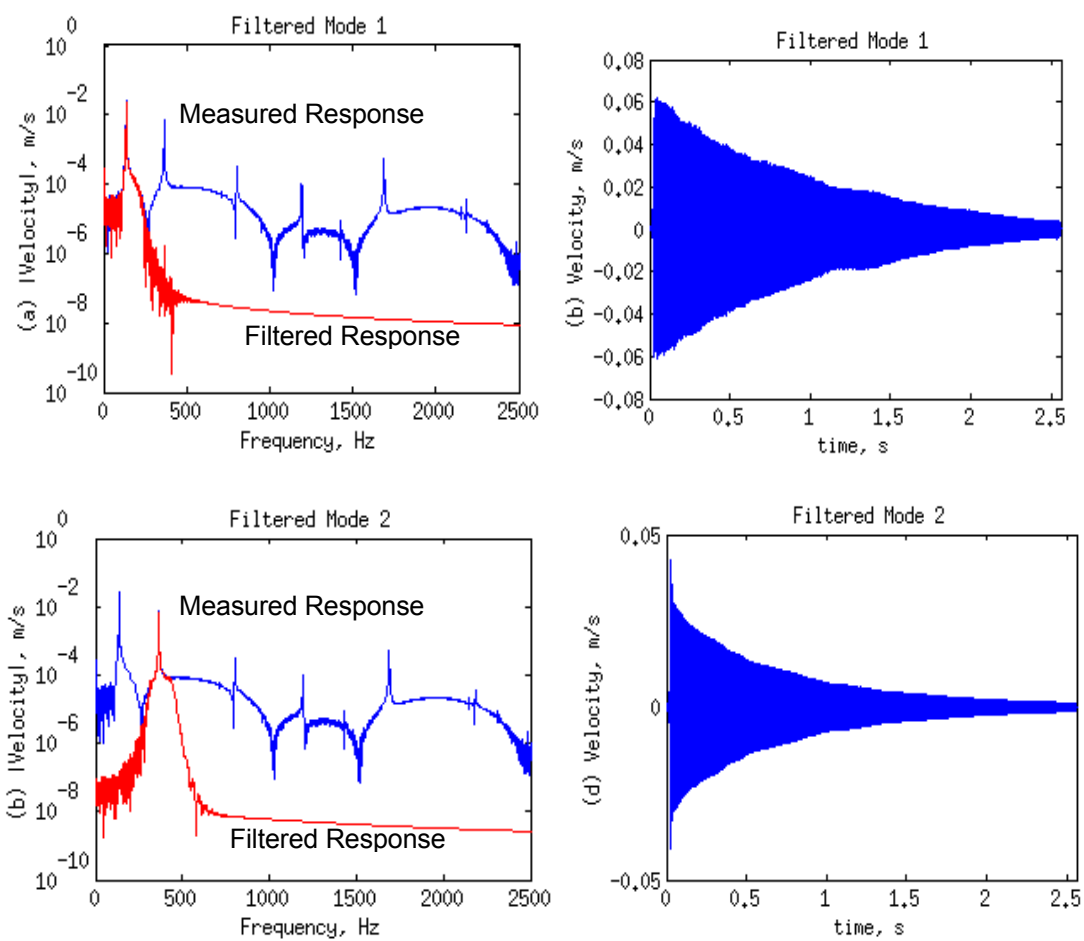


Figure 11: Single mode filtering of the free velocity response of point 28: (a) 10th order low-pass Butterworth filter for Mode 1 with cutoff frequency of 240 Hz; (b) filtered time domain response of Mode 1; (c) 5th order band-pass Butterworth filter for Mode 2 with cutoff frequencies 300 Hz and 450 Hz; (d) filtered time domain response of Mode 2

The single mode filter approach effectively isolates a single mode and produced a mono-component time domain signal for both the two modes that are shown. This could be applied to most of the modes in the free velocity response, especially since the modes are well separated. For a structure with close modes, a different approach may be needed. For example a band of close modes could first be isolated using a band-pass filter similar to the one used for Mode 2 above. Then, one might try Empirical Mode Decomposition on the resulting signal, and it may be more effective since the overall number of modes in the band is likely to be much fewer than the measured signal. These ideas are being explored for future work.

3.4.3 Hilbert Transform with Curve Fitting

Once one has isolated mono-component signals from the measured response, the Hilbert transform curve fitting approach described in Section 2.2 can be applied to extract the nonlinear time dependent properties of the system. First, the phase signal from Eq. (6) is fit with a 5th degree polynomial. The time derivative of the polynomial fit is equal to the damped natural frequency, and this can be formed with Eq. (11). Then, the amplitude of the Hilbert transformed signal can be fit with a cubic polynomial in order to extract the time dependent damping. Figure 12 shows the Hilbert transformed velocity Amplitude (a) and phase (b) as well as the curve fits of those signals. Figure 13 shows the time dependent natural frequency and damping that were

extracted from the curve fits. The natural frequency changes by less than 1% over the course of the free response, however, this is likely spurious since the modes were found to be predominantly linear in frequency. The damping changes a significant amount over time, and as shown in Fig. (14), the damping is clearly nonlinear since it is a function of the amplitude of the response. The same procedure can be followed for the filtered signal of Mode 2. The damping-amplitude relationship of Mode 2 is plotted in Fig. (15).

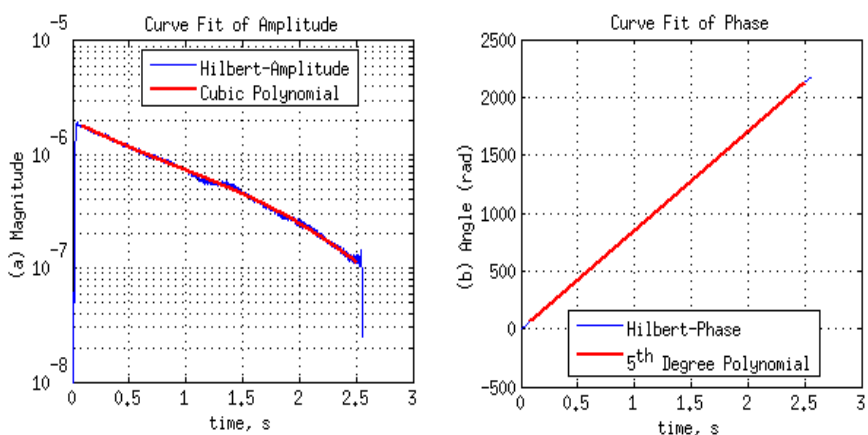


Figure 12: Curve fit of the amplitude(a) and phase(b) of the Hilbert transform of the filtered Mode 1

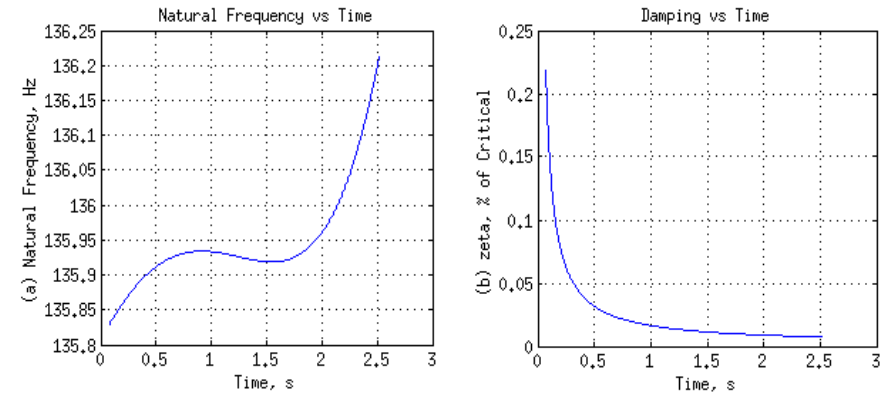


Figure 13: Time varying natural frequency and damping that were extracted from the curve fits in Fig. (12)

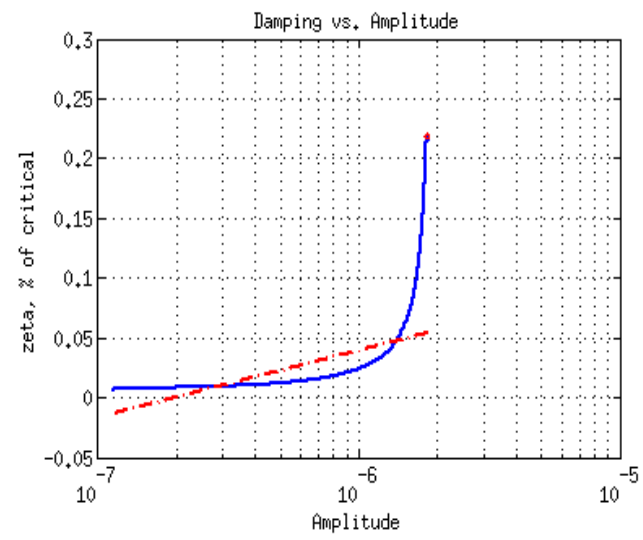


Figure 14: Nonlinear damping plotted versus the amplitude of the Hilbert transformed signal of Mode 1

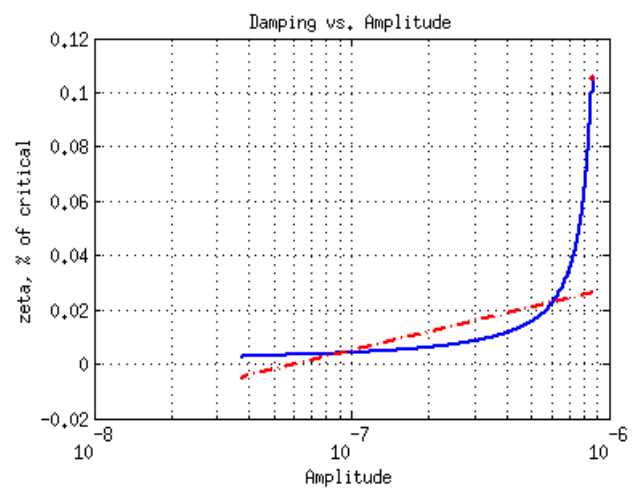


Figure 15: Nonlinear damping plotted versus the amplitude of the Hilbert transformed signal of Mode 2

3.4.4 Discussion

The Empirical Mode Decomposition method and the single mode filtering method were both used to isolate monocomponent signals from the measured response. The single mode filtering method was found to produce very clean signals with a single, distinct frequency component. The identified nonlinear damping functions had clear amplitude dependence, and those functions were different due to the differences in filtered modes. Since the beam has well spaced modes, the single mode filtering approach could be used to identify the nonlinear damping functions on the remainder of the modes. For other systems with closely space modes, a combination of bandpass filtering and Empirical Mode Decomposition may produce the mono-component signals needed to apply the Hilbert transform curve fitting method. In any event, it seems that these tools can be readily applied to characterize the damping nonlinearity in this structure.

4. Conclusions

This paper reviewed a few methods for system identification of nonlinear systems with slowly time-varying nonlinear properties, especially damping. In particular, the Empirical Mode Decomposition method was compared with a method based on band-pass filtering around each resonance, in order to obtain single mode responses that could be processed using the Hilbert transform. The Zeroed Early-Time FFT (ZEFFT) was also discussed and applied to the measurements, and was found to allow one to quickly and quite robustly identify which modes had natural frequencies that were amplitude dependent. That method was not explored further in this work, although it might be helpful in obtaining more quantitative results in the future. The Hilbert transform method seemed to provide the most convenient approach for quantifying the dependence of the frequency and damping on time (and hence amplitude), however the signal of interest must be first decomposed into moncomponent signals. The Empirical Mode Decomposition method and a band-pass filtering method were both used, but the former gave quite unsatisfactory results and was not pursued further. This may not be a fault of the algorithm; the authors are certainly not experts and were at the mercy of a particular implementation of the EMD method. On the other hand, simple band-pass filtering was quite effective for the system considered here, although it is difficult to be sure that the filter has not distorted the signal of interest. In any event, once a mono-component response was available the Hilbert transform method was quite effective.

The proposed methods were applied to free velocity response measurements of a linked-beam system that contains bolted joints. The ZEFFTs of the measured responses showed little sign of variation in the natural frequencies of the modes, and this seems to imply that the stiffness of the system is predominantly linear. Therefore, linear modal analysis was performed at different torque values to assess any trends in damping versus torque. Some trends were clearly observed but it is difficult to assess the accuracy of the damping measurement in each configuration and to determine whether the trends observed, where damping both increased and decreased with increasing torque, were meaningful. The measurements were then processed with Empirical Mode Decomposition and with band-pass filtering in order to isolate individual modes. The Empirical Mode Decomposition method was not successful in extracting mono-component signals from the measurements, perhaps because so many modes were excited in the free response. The band-pass filtering approach worked very well to isolate mono-component signals, since this system has well spaced modes. Once the modes were

isolated, the Hilbert transform curve fit approach identified significantly nonlinear damping from the measurements, and the damping-amplitude relationships were displayed. Despite the initial success of the bandpass filtering and Hilbert transform approach, all of the methods are being investigated further to understand which methods work best in a variety of situations.

Acknowledgment

Sandia National Laboratories is a multi-program laboratory managed and operated by Sandia Corporation, a wholly owned subsidiary of Lockheed Martin Corporation, for the U.S. Department of Energy's National Nuclear Security Administration under contract DE-AC04-94AL85000.

References

- [1] P. F. Pai, "Instantaneous Frequency of an Arbitrary Signal," *International Journal of Mechanical Sciences*, vol. 52, pp. 1682-1693, 2010.
- [2] M. Feldman, "Non-Linear Free Vibration Identification via the Hilbert Transform," *Journal of Sound and Vibration*, vol. 208, pp. 475-489, 1997.
- [3] M. Feldman, "Hilbert Transform in Vibration Analysis," *Mechanical Systems and Signal Processing,* vol. 25, pp. 735-802, 2011.
- [4] N. E. Huang, *et al.*, "The empirical mode decomposition and the Hilbert spectrum for nonlinear and nonstationary time series analysis," in *Proc R Soc Lond A*, 1998, pp. 903-995.
- [5] G. Kerschen, et al., "Toward a Fundamental Understanding of the Hilbert-Huang Transform in Nonlinear Structural Dynamics," *Journal of Vibration and Control*, vol. 14, pp. 77-105, 2008.
- [6] L. Heller, et al., "Experimental Identification of Nonlinear Dynamic Properties of Built-up Structures," Journal of Sound and Vibration, vol. 327, 2009.
- [7] D. Celic and M. Boltezar, "Identification of Dynamic Properties of Joints Using Frequency-Response Functions," *Journal of Sound and Vibration*, vol. 317, pp. 158-174, 2008.
- [8] W.-J. Kim, et al., "Non-linear Joint Parameter Identification Using the Frequency Reponse Function of the Linear Substructure" *Journal of Mechanical Engineering Science*, vol. 218, pp. 947-955, 2004.
- [9] Y. Ren and C. F. Beards, "Identification of Joint Properties of a Structure using FRF Data," *Journal of Sound and Vibration*, vol. 186, pp. 567-587, 1995.
- [10] J.-S. Tsai and Y.-F. Chou, "The Identification of Damping Characteristics of a Single Bolt Joint," *Journal of Sound and Vibration*, vol. 125, pp. 487-502, 1988.
- [11] H. Sumali and R. A. Kellogg, "Calculating Damping From Ring-Down Using Hilbert Transform and Curve Fitting," presented at the 4th International Operational Modal Analysis Conference (IOMAC), Istanbul, Turkey, 2011.
- [12] M. W. Sracic and M. S. Allen, "Method for Identifying Models of Nonlinear Systems Using Linear Time Periodic Approximations," *Mechanical Systems and Signal Processing*, vol. 25, pp. 2705–2721, 2011.
- [13] S. Tsakirtzis, et al., "Modelling of Nonlinear Modal Interactions in the Transient Dynamics of an Elastic Rod with an Essentially Nonlinear Attachment," *Commun Nonlinear Sci Numer Simulat*, vol. 15, pp. 2617-2633, 2010.
- [14] M. S. Allen and R. L. Mayes, "Estimating the Degree of Nonlinearity in Transient Responses With Zeroed Early-Time Fast Fourier Transforms," *Mechanical Systems and Signal Processing*, vol. 24, pp. 2049-2064, 2010.
- [15] N. E. Huang and Z. Wu, "A Review on Hilbert-Huang Transform: Method and its Applications to Geophysical Studies," *Reviews of Geophysics*, vol. 46, 2008.
- [16] R. T. Rato, et al., "On the HHT, its problems and some solutions," *Mechanical Systems and Signal Processing*, vol. 22, pp. 1374-1394, 2008.

Appendix 1: Linear Curve Fitting of the 9 Nm data with ATA Engineering's AFPoly

Mode shapes and "Stability Diagram" are shown below. Modal Indicator Function (curve) # Shape and pole orders (squares or triangles) 1 2 T1 3 4 4c T2 5 6 T3 A1 T4 **A**+ B-C-B+ C-B1 7 T5 8 T6 7b 9